Electronic structure of paramagnetic $In_{1-x}Mn_x$ As nanowires

X.W. Zhang[a] and J.B. Xia

Chinese Center of Advanced Science and Technology (World Laboratory), P.O. Box 8730, Beijing 100080, P.R. China
and
Institute of Semiconductors, Chinese Academy of Sciences, P.O. Box 912, Beijing 100083, P.R. China

Abstract. The electronic structure, spin splitting energies, and g factors of paramagnetic $In_{1-x}Mn_xAs$ nanowires under magnetic and electric fields are investigated theoretically including the sp-d exchange interaction between the carriers and the magnetic ion. We find that the effective g factor changes dramatically with the magnetic field. The spin splitting due to the sp-d exchange interaction counteracts the Zeeman spin splitting. The effective g factor can be tuned to zero by the external magnetic field. There is also spin splitting under an electric field due to the Rashba spin-orbit coupling which is a relativistic effect. The spin-degenerated bands split at nonzero k_z (k_z is the wave vector in the wire direction), and the spin-splitting bands cross at $k_z = 0$, whose k_z-positive part and negative part are symmetrical. A proper magnetic field makes the k_z-positive part and negative part of the bands asymmetrical, and the bands cross at nonzero k_z. In the absence of magnetic field, the electron Rashba coefficient increases almost linearly with the electric field, while the hole Rashba coefficient increases at first and then decreases as the electric field increases. The hole Rashba coefficient can be tuned to zero by the electric field.

PACS. 72.25.Dc Spin polarized transport in semiconductors – 73.21.Hb Quantum wires – 75.75.+a Magnetic properties of nanostructures

1 Introduction

Nowadays, much of the research in semiconductor physics has been shifting towards diluted magnetic semiconductors (DMS) [1–6], as well as their nanostructures [7–14]. These DMS systems can perform spin-dependent effect on electron spin, so have extensive application in spintronics [15,16]. Meanwhile, there has been a growing interest and experimental progress in the one-dimensional semiconductors, which are called nanowires. Nanowires can be grown out of numerous semiconductor materials with a large range of radii and by several methods [17–23]. Especially, Mn-doped semiconductor nanowires were well synthesized [12–14]. The electronic structure and other properties of DMS nanostructures were studied extensively [7,11–13]. The magnetic field tunable g factor in DMS quantum dots was investigated theoretically [11]. It is expected that the magnetic field tunable g factor will also happen in DMS nanowires.

There is another important spin-dependent effect, named Rashba spin-orbit coupling, which is also widely investigated [24–27]. Based on these spin-dependent effects, electron spin might be used in the future to build quantum computing devices that combine logic and storage functions. One of the most important spin-based devices was proposed by Datta and Das [28], which makes use of the Rashba spin-orbit coupling in order to perform controlled rotations of a field-effect transistor (FET) [29]. The Datta-Das device also uses diluted magnetic semiconductors as Source and Drain.

Recently, people have been paying special attention to the Rashba spin-orbit coupling in semiconductor nanowires [30–40] because of its abundance of physical phenomena. The Rashba spin-orbit splitting [31–37] and spin-polarized transport properties [38–40] of nanowires have been studied theoretically. However, the spin splitting under both magnetic field and electric field in paramagnetic nanowires and the hole Rashba effect of nanowires are not clear.

In this paper, we use the eight-band effective-mass model of semiconductor nanowires, taking into account the sp-d exchange interaction, to study the electronic structure, spin splitting energies, and g factors of paramagnetic $In_{1-x}Mn_xAs$ nanowires under magnetic and electric fields. The remainder of this paper is organized as follows. The calculation model is given in Section 2. The results and discussion are given in Section 3. Section 4 is the conclusion.

[a] e-mail: `zhxw99@semi.ac.cn`

2 Theoretical model and calculations

In the absence of external fields, we represent the eight-band effective-mass Hamiltonian in the Bloch function bases $|S\rangle \uparrow, |11\rangle \uparrow, |10\rangle \uparrow, |1-1\rangle \uparrow, |S\rangle \downarrow, |11\rangle \downarrow, |10\rangle \downarrow, |1-1\rangle \downarrow$ as

$$H_{eb} = \begin{pmatrix} H_{int} & \\ & H_{int} \end{pmatrix} + H_{so}. \tag{1}$$

H_{so} is the valence band spin-orbit coupling Hamiltonian which was given before [41,42]. H_{int} is written as

$$H_{int} = \frac{1}{2m_0} \begin{pmatrix} \epsilon_g + P_e & \frac{i}{\sqrt{2}}p_0p_+ & ip_0p_z & \frac{i}{\sqrt{2}}p_0p_- \\ -\frac{i}{\sqrt{2}}p_0p_- & -P_1 & -S & -T \\ -ip_0p_z & -S^\star & -P_3 & -S \\ -\frac{i}{\sqrt{2}}p_0p_+ & -T^\star & -S^\star & -P_1 \end{pmatrix}, \tag{2}$$

where

$$P_e = \alpha p_- p_+ + \alpha p_z^2, \tag{3a}$$

$$P_1 = \frac{L' + M'}{2} p_- p_+ + M' p_z^2, \tag{3b}$$

$$P_3 = M' p_- p_+ + L' p_z^2, \tag{3c}$$

$$T = \frac{L' - M' - N'}{4} p_+^2 + \frac{L' - M' + N'}{4} p_-^2, \tag{3d}$$

$$T^* = \frac{L' - M' - N'}{4} p_-^2 + \frac{L' - M' + N'}{4} p_+^2, \tag{3e}$$

$$S = \frac{1}{\sqrt{2}} N' p_- p_z, \tag{3f}$$

$$S^* = \frac{1}{\sqrt{2}} N' p_+ p_z, \tag{3g}$$

$$p_\pm = p_x \pm i p_y. \tag{3h}$$

$\epsilon_g = 2m_0 E_g$, E_g is the bandgap of the bulk material, $p_0 = \sqrt{2m_0 E_P}$, and E_P is the matrix element of Kane's theory. α, L', M', N' are the effective mass parameters. Since we have taken into account the coupling of the valence band and the conduction band, we should subtract the contribution of the conduction band from the Luttinger parameters L and N, that is to say, $L' = L - E_P/E_g$, $N' = N - E_P/E_g$. M does not change, and $M' = M$. We should also subtract the contribution of the valence band from the electron effective mass [41],

$$\alpha = \frac{m_0}{m_c} - \frac{E_P}{3} \left(\frac{2}{E_g} + \frac{1}{E_g + \Delta_{so}} \right), \tag{4}$$

where m_c is the electron effective mass and Δ_{so} is the spin-orbit splitting energy of the valence band.

We assume that the electric field is applied along the y-direction. The electric field potential term is written as

$$V = e\mathbf{F} \cdot \mathbf{r} = eFy = eFr\sin\theta = -\frac{i}{2}eFre^{i\theta} + \frac{i}{2}eFre^{-i\theta}. \tag{5}$$

We also assume that the magnetic field is along the x-direction. In the absence of magnetic ions, the magnetic field brings three terms in the Hamiltonian, the antisymmetric term H_{asym} [43], magnetic-momentum term

H_{mm} [44], and spin-Zeeman-splitting term H_{Zeeman}. In the presence of magnetic ions (Mn^{2+}), the magnetic field also brings the magnetization of the localized spins, so brings two other terms in the Hamiltonian, s-d and p-d exchange interaction terms between the carriers and the magnetic ion, H_{sd} and H_{pd}, which are written as [6]

$$H_{sd} = \alpha \mathbf{s}_e \cdot \mathbf{M}/(g_{\mathrm{Mn}}\mu_B), \tag{6}$$

$$H_{pd} = \beta \mathbf{s}_h \cdot \mathbf{M}/(g_{\mathrm{Mn}}\mu_B), \tag{7}$$

$g_{Mn} = 2$ is the g factor of magnetic ion, $\mathbf{s}_e(\mathbf{s}_h)$ is the spin ($s_e = s_h = \frac{1}{2}$) of electron (hole), αN_0 and βN_0 are the s-d and p-d exchange constants, N_0 is the number of cations per unit volume, the exchange constants of $\mathrm{In}_{1-x}\mathrm{Mn}x\mathrm{As}$ are cited from reference [3], $\mathbf{M}$ is the magnetization of the localized spins of the magnetic ions. In the paramagnetic case, $\mathbf{M}$ is parallel with the external magnetic field, the magnitude of $\mathbf{M}$ is given by [6]

$$M = S g_{\mathrm{Mn}}\mu_B N_0 x_{eff} B_S \left[\frac{S g_{\mathrm{Mn}}\mu_B B}{k_B(T + T_{AF})} \right], \tag{8}$$

where $S = \frac{5}{2}$ is the spin of magnetic ion, x_{eff} is the effective content of magnetic ions, T_{AF} accounts for the reduced single-ion contribution due to the anti-ferromagnetic Mn-Mn coupling, and the Brillouin function $B_S(x)$ is

$$B_S(x) = \frac{2S+1}{2S} \coth\left(\frac{2S+1}{2S} x \right) - \frac{1}{2S} \coth\left(\frac{1}{2S} x \right). \tag{9}$$

For $\mathrm{In}_{1-x}\mathrm{Mn}_x\mathrm{As}$, $x_{eff} = x$ and $T_{AF} = 0$ [6]. The whole Hamiltonian in the presence of electric and magnetic fields is written as

$$H = H_{eb} + V + H_{asym} + H_{mm} + H_{Zeeman} + H_{sd} + H_{pd}. \tag{10}$$

We assume that the nanowires have cylindrical symmetry, the longitudinal axis is along the z direction, and the electrons and holes are confined laterally in an infinitely high potential barrier. The longitudinal wave function is the plane wave, and the lateral wave function is expanded in Bessel functions. The total envelope function including the electron and hole states is

$$\Psi_{J,k_z} = \sum_n \begin{pmatrix} e_{l,n,\uparrow} A_{l,n} J_l\left(k_n^l r\right) e^{il\theta} \\ b_{l-1,n,\uparrow} A_{l-1,n} J_{l-1}\left(k_n^{l-1} r\right) e^{i(l-1)\theta} \\ c_{l,n,\uparrow} A_{l,n} J_l\left(k_n^l r\right) e^{il\theta} \\ d_{l+1,n,\uparrow} A_{l+1,n} J_{l+1}\left(k_n^{l+1} r\right) e^{i(l+1)\theta} \\ e_{l+1,n,\downarrow} A_{l+1,n} J_{l+1}\left(k_n^{l+1} r\right) e^{i(l+1)\theta} \\ b_{l,n,\downarrow} A_{l,n} J_l\left(k_n^l r\right) e^{il\theta} \\ c_{l+1,n,\downarrow} A_{l+1,n} J_{l+1}\left(k_n^{l+1} r\right) e^{i(l+1)\theta} \\ d_{l+2,n,\downarrow} A_{l+2,n} J_{l+2}\left(k_n^{l+2} r\right) e^{i(l+2)\theta} \end{pmatrix} e^{ik_z z}, \tag{11}$$

where $J = l + 1/2$ is the total angular momentum and $A_{l,n}$ is the normalization constant,

$$A_{l,n} = \frac{1}{\sqrt{\pi} R J_{l+1}\left(\alpha_n^l\right)}. \tag{12}$$

Table 1. The parameters of InAs used in this paper.

m_c	L	M	N	κ	E_P(eV)	E_g(eV)	Δ_{so}(eV)	ϵ_r
0.02226	54.2	3.87	55.6	7.68	21.6	0.418	0.38	15.15

$\alpha_n^l = k_n^l R$ is the nth zero point of $J_l(x)$, R is the radius of the wire, and k_z is the wave vector along the wire direction, which is a good quantum number. In calculating the matrix elements of the Hamiltonian we can use the properties of the operators $p_\pm$,

$$p_\pm J_l(kr) e^{il\theta} = \mp \frac{\hbar}{i} k J_{l\pm1}(kr) e^{i(l\pm1)\theta}. \quad (13)$$

3 Results and discussion

In this section, we calculate the electronic structure, spin splitting energies, and g factors of paramagnetic In$_{1-x}$Mn$_x$ As nanowires under magnetic and electric fields using the eight-band effective-mass model. The parameters of InAs [45] used in this paper are listed in Table 1. However, these parameters measured in the bulk material include some contributions, say, nonlocal character of the self-consistent potential, that are absent in narrow-gap nanostructures [41]. Therefore, using these parameters requires taking special precautions. The nonlocal contributions are

$$\Delta L = -21\delta_{nl}, \ \Delta M = 3\delta_{nl}, \ \Delta N = -24\delta_{nl}, \quad (14)$$

$$\Delta \alpha = -10\delta_{nl}, \ \delta_{nl} = \frac{2}{15\pi\epsilon_r E_g}\sqrt{\frac{E_B E_p}{3}}, \quad (15)$$

where $E_B = 27.211$ eV and ϵ_r is the dielectric constant given in Table 1.

Figure 1 shows the electron (a) and hole states (b) of In$_{1-x}$Mn$_x$As nanowires with $R = 18$ nm and $x = 0.005$ under magnetic field $B = 1.5$ T ($B||x$) at $T = 10$ K as functions of k_z. The symbol of each energy level represents the main components of it's wave function. For example, $(1,0)S \uparrow$ means that the state consists mainly of the $n = 1$, $l = 0$ state of the effective-mass envelope function multiplied with the S Bloch state of the conduction-band bottom and the spin-up state. The magnetic field brings the magnetization of the localized spins of the magnetic ions which affects the states of carriers via the sp-d exchange interaction between the carriers and the magnetic ion and leading to a spin splitting. The magnetic field also brings the Zeeman spin splitting. All the spin splitting has the form $H_{spin} \sim \sigma_x$ [see Eq. (10)]. So the spin states in Figure 1 are almost the eigenstates of σ_x.

We show the spin splitting energies in three cases of In$_{1-x}$Mn$_x$As nanowires with $R = 18$ nm and $x = 0.005$ at $k_z = 0$ and $T = 10$ K as functions of B ($B||x$) in Figure 2a. In "not diluted" case (dashed line), $x = 0$ and the spin splitting is only due to the Zeeman splitting. As the g factor is negative, the spin splitting energy is negative, whose inverse is shown by the dashed line. The "M only" case (dotted line) is a dummy case in which the
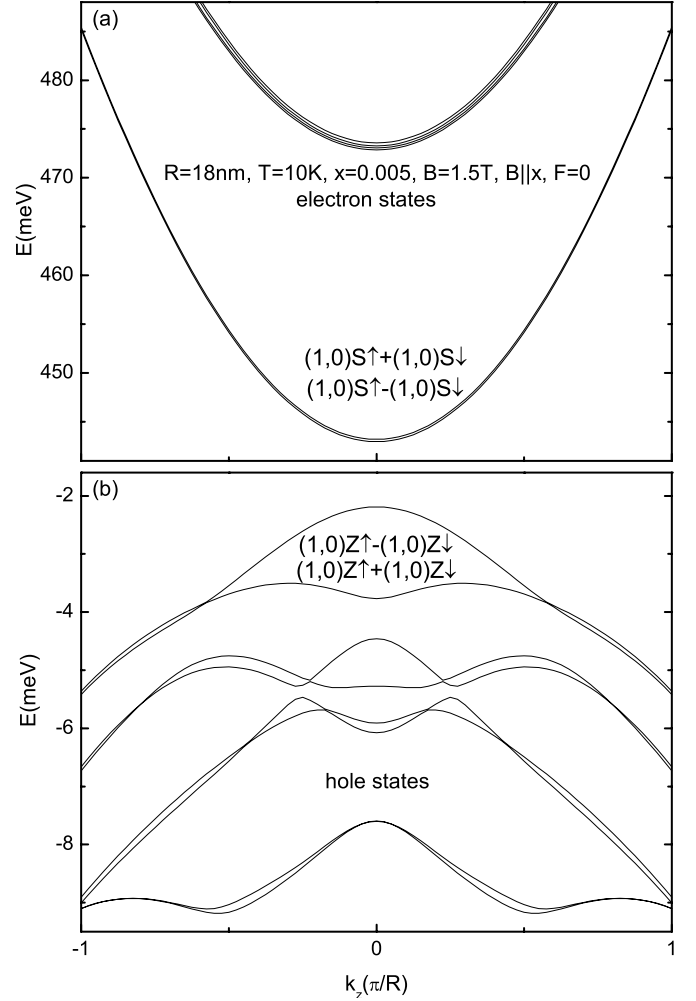
Fig. 1. (a) Electron states of In$_{1-x}$Mn$_x$As nanowires with $R = 18$ nm and $x = 0.005$ under magnetic field $B = 1.5$ T ($B||x$) at $T = 10$ K as functions of k_z. (b) Hole states of In$_{1-x}$Mn$_x$As nanowires with $R = 18$ nm and $x = 0.005$ under magnetic field $B = 1.5$ T ($B||x$) at $T = 10$ K as functions of k_z.

magnetic field only brings the magnetization of the localized spins of the magnetic ions, whose other effects are ignored, then the spin splitting is only due to the sp-d exchange interaction between the carriers and the magnetic ion. The "diluted" case (bold solid line) is the real case of In$_{1-x}$Mn$_x$ As nanowires investigated in the paper, in which the spin splitting due to the sp-d exchange interaction counteracts the Zeeman spin splitting. The absolute value of Zeeman spin splitting energy (dashed line) increases with the magnetic field almost linearly, while the exchange spin splitting energy (dotted line) increases and saturates as the magnetic field increases due to the saturation of the magnetization of the localized spins. The dashed line and dotted line cross at about $B = 5$ T. The whole spin splitting energy (bold solid line) is the sum of all the spin splitting energies. We see from Figure 2a that the bold solid line is approximately equals the dotted line subtracts the dashed line which means the sum of these two spin splitting energies, but not exactly, for example,
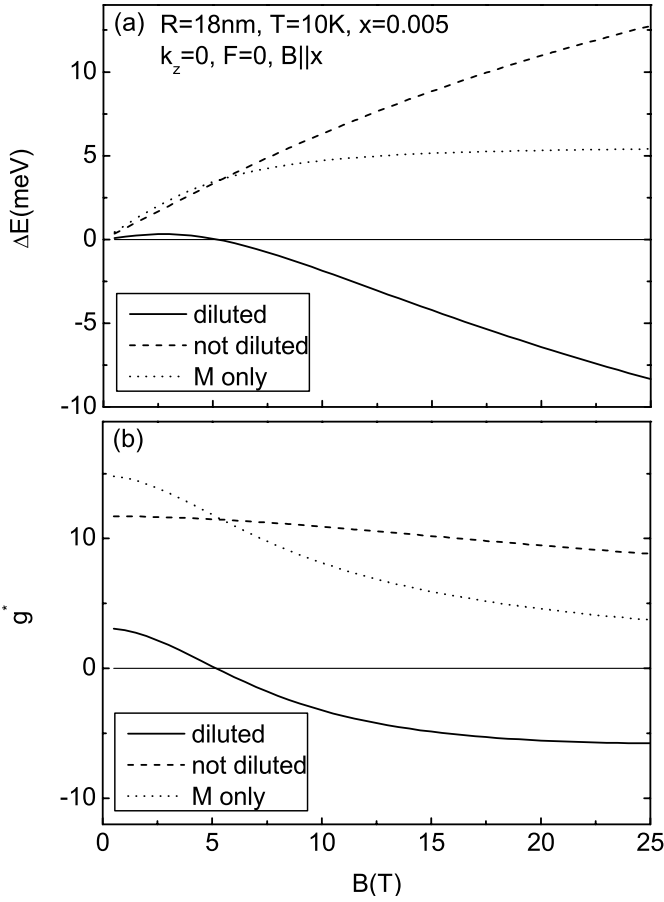
Fig. 2. (a) Spin splitting energies [spin-up (in x-direction) energy subtracts spin-down energy] of $In_{1-x}Mn_xAs$ nanowires with $R = 18$ nm and $x = 0.005$ at $k_z = 0$ and $T = 10$ K as functions of B ($B||x$). (b) Effective g factors of $In_{1-x}Mn_xAs$ nanowires with $R = 18$ nm and $x = 0.005$ at $k_z = 0$ and $T = 10$ K as functions of B ($B||x$).

Fig. 3. (a) Electron states of $In_{1-x}Mn_xAs$ nanowires with $R = 18$ nm under electric field $F = 15$ mV/nm ($F||y$) as functions of k_z. (b) Electron states of $In_{1-x}Mn_xAs$ nanowires with $R = 18$ nm and $x = 0.005$ under electric field $F = 15$ mV/nm ($F||y$) and magnetic field $B = 1.5$ T ($B||x$) at $T = 10$ K as functions of k_z. (c) Spin splitting energies of $In_{1-x}Mn_xAs$ nanowires with $R = 18$ nm and $x = 0.005$ under electric field $F = 15$ mV/nm ($F||y$) and magnetic field $B = 1.5$ T ($B||x$) at $T = 10$ K as functions of k_z. "F", "B", "FB" indicate the presence of electric field only, magnetic field only, both electric and magnetic fields. (d) Hole states of $In_{1-x}Mn_xAs$ nanowires with $R = 18$ nm under electric field $F = 15$ mV/nm ($F||y$) as functions of k_z. Inset: spin splitting energy of the hole states.

the cross point of the bold solid line and the thin solid line (zero line) is on the left of the cross point of the dotted line and the dashed line, due to the combined effect of the exchange spin splitting and Zeeman spin splitting.

For each of the cases in Figure 2a, we assume a effective spin Hamiltonian $H_{spin} = \frac{1}{2}g^*\mu_B\sigma_x B$, then the spin splitting energy is $\Delta E = g^*\mu_B B$ and the effective g factor is $g^* = \frac{\Delta E}{\mu_B B}$. We show the g factors in the above three cases in Figure 2b. Correspondingly, the dashed is the absolute value of the "not diluted" g factor. The g factor of the lowest electron states of InAs nanostructures is in the range of $[-\infty, 2]$ [42], so the g factor in "not diluted" case (dashed line) can not be about 10 but be about -10. The g factor due to exchange spin splitting (dotted line) is always positive because there is a ferromagnetic interaction between the electron and the magnetic ion [see Eq. (6)]. The bold solid line shows that the effective g factor in the real case under $B = 1.5$ T is positive, which is confirmed by the state components in Figure 1a. Corresponding to Figure 2a, the bold solid line is approximately equals the dotted line subtracts the dashed line in Figure 2b. It is

noticed to find that the effective g factor can be tuned to zero by an external magnetic field, which means that the spin does not split at a proper magnetic field.

It is known that a transverse electric field can bring spin splitting in semiconductor nanowires [46]. From Figure 3a, we see that the two spin bands split at $k_z \neq 0$, which cross at $k_z = 0$. The k_z-positive part and negative part of the bands are symmetrical. When we applied a magnetic field along x-direction, as shown in Figure 3b, the k_z-positive part and negative part of the bands becomes asymmetrical, the two bands cross at $k_z > 0$. We show the spin splitting energies in the above two cases [Figs. 3a and 3b, indicated by 'F' and 'FB', respectively] and the case in Figure 1a which is indicated by 'B'. The spin splitting energy in Figure 1a is always positive. But the spin splitting energies in Figures 3a and 3b change from positive values to negative values with k_z, as the two bands cross. The bold solid line and dotted line are the inverse spin splitting energies. We see from the bold solid line that there is a linear relationship between the spin splitting energy and k_z when k_z is small. It is well-known that the k-linear Rashba term is written
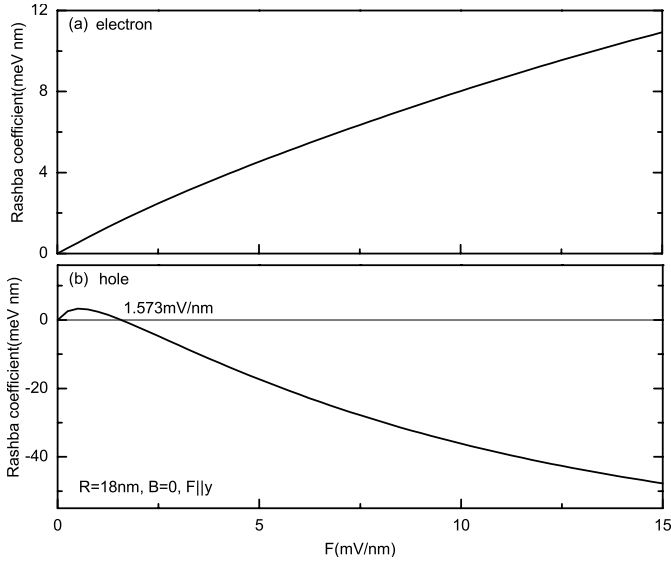
Fig. 4. (a) Electron Rashba coefficient of In$_{1-x}$Mn$_x$As nanowires with $R = 18$ nm as a function of F ($F||y$). (b) Hole Rashba coefficient of In$_{1-x}$Mn$_x$As nanowires with $R = 18$ nm as a function of F ($F||y$).

as $H_{Ra} = \gamma\sigma \cdot (\mathbf{k} \times \hat{\mathbf{F}})$, where γ is the Rashba coefficient and $\hat{\mathbf{F}}$ is the unit vector along the electric field direction. In the case of Figure 3a, $H_{Ra} = -\gamma k_z \sigma_x$, and $\gamma > 0$. And the spin splitting term due to the magnetic field along x direction is $\frac{1}{2}g^*\mu_B B\sigma$, and g^* is positive [see Fig. 1a and the dashed line in Fig. 3c]. The whole spin Hamiltonian in the case of Figure 3b is approximately $H_{spin} = (-\gamma k_z + \frac{1}{2}g^*\mu_B B)\sigma_x$. So there is a positive k_z (about $\frac{\frac{1}{2}g^*\mu_B B}{\gamma}$) at which $H_{spin} = 0$. And the energy bands are asymmetrical. We also show the hole states and spin splitting energy in the absence of magnetic field under transverse electric field in Figure 3d. The splitting energy is also a linear function of k_z when k_z is small. So we can define the same k-linear Rashba term and Rashba coefficient of the hole as those of the electron. We see from the state components in Figure 4d that when $k_z > 0$, the spin-down (in x-direction) state is below the spin-up state. This is contrary to the the case in Figure 3a, so the hole Rashba coefficient in the case of Figure 4d is negative.

The electron (a) and hole (b) Rashba coefficients of In$_{1-x}$Mn$_x$As nanowires with $R = 18$ nm as functions of F ($F||y$) are shown in Figure 4. We see that the electron Rashba coefficient increases almost linearly with the electric field. While the hole Rashba coefficient increases at first and then decreases as the electric field increases, because the hole states changes dramatically with the electric field which can be seen from the state components of Figure 1b and Figure 3d whose highest hole states are quite different. The hole bands are very close to each other, so the electric field can easily couple them. On the contrary, the lowest electron bands are far away from the upper electron bands. It is noticed to find that the hole Rashba coefficient can be tuned to zero by an external electric field, and we can change the sign of the hole

Rashba coefficient by changing the strength of the external electric field without changing its direction.

4 Conclusions

The electronic structure, spin splitting, and g factors of paramagnetic In$_{1-x}$Mn$_x$As nanowires are investigated theoretically. We find that the effective g factor changes dramatically with the magnetic field. The spin splitting due to the sp-d exchange interaction counteracts the Zeeman spin splitting. The effective g factor can be tuned to zero by the external magnetic field. There is also spin splitting under an electric field due to the Rashba spin-orbit coupling which is a relativistic effect. The spin-degenerated bands split at nonzero k_z (k_z is the wave vector in the wire direction), and the spin-splitting bands cross at $k_z = 0$, whose k_z-positive part and negative part are symmetrical. A proper magnetic field makes the k_z-positive part and negative part of the bands asymmetrical, and the bands cross at nonzero k_z. The spin splitting due to the electric field also counteracts the spin splitting due to the magnetic field. In the absence of magnetic field, the electron Rashba coefficient increases almost linearly with the electric field, while the hole Rashba coefficient increases at first and then decreases as the electric field increases. The hole Rashba coefficient can be tuned to zero by the electric field. We can change the sign of the hole Rashba coefficient by changing the strength of the external electric field without changing its direction.

References

1. K. Huang, B.W. Wessels, Appl. Phys. Lett. **52**, 1155 (1988)
2. S.J. May, A.J. Blattner, B.W. Wessels, Phys. Rev. B **70**, 073303 (2004)
3. G.D. Sanders, Y. Sun, F.V. Kyrychenko, G.A. Khodaparast, M.A. Zudov, J. Kono C.J. Stanton, Y.H. Matsuda, N. Miura, H. Munekata, Phys. Rev. B **68**, 165205 (2003)
4. J. Wang, C. Sun, J. Kono, A. Oiwa, H. Munekata, L. Cywinski, L.J. Sham, Phys. Rev. Lett. **95**, 167401 (2005)
5. H. Akai, Phys. Rev. Lett. **81**, 3002 (1998)
6. T. Dietl, H. Ohno, F. Matsukura, Phys. Rev. B **63**, 195205 (2001)
7. Y.H. Matsuda, G.A. Khodaparast, M.A. Zudov, J. Kono, Y. Sun, F.V. Kyrychenko, G.D. Sanders, C.J. Stanton, N. Miura, S. Ikeda, Y. Hashimoto, H. Munekata, Phys. Rev. B **70**, 195211 (2004)
8. G.A. Khodaparast, M.A. Zudov, J. Kono, Y.H. Matsuda, T. Ikaida, S. Ikeda, N. Miura, T. Slupinski, A. Oiwa, H. Munekata, G.D. Sanders, Y. Sun, C.J. Stanton, J. Supercond. **16**, 107 (2003)

9. S. Chakrabarti, M.A. Holub, P. Bhattacharya, T.D. Mishima, M.B. Santos, M.B. Johnson, D.A. Blom, Nano Lett. **5**, 209 (2005)
10. M. Holub, S. Chakrabarti, S. Fathpour, Y. Lei, S. Ghosh, Appl. Phys. Lett. **85**, 973 (2004)
11. Kai Chang, J.B. Xia, F.M. Peeters, Appl. Phys. Lett. **82**, 2661 (2003)
12. P.V. Radovanovic, C.J. Barrelet, S. Gradecak, F. Qian, C.M. Lieber, Nano Lett. **5**, 1407 (2005)
13. P. Mock, T. Topuria, N.D. Browning, G.R. Booker, N.J. Mason, R.J. Nicholas, M. Dobrowolska, S. Lee, J.K. Furdyna, Appl. Phys. Lett. **79**, 946 (2001)
14. S.P. Guo, A. Shen, H. Yasuda, Y. Ohno, F. Matsukura, H. Ohno, J. Cryst. Growth **208**, 799 (2000)
15. G.A. Prinz, Science **282**, 1660 (1998)
16. S.A. Wolf et al., Science **294**, 1488 (2001); *Semiconductor Spintronics and Quantum Computation*, edited by D.D. Awschalom, D. Loss, N. Samarth (Springer, Berlin, 2002)
17. M. Law, J. Goldberger, P. Yang, Annu. Rev. Mater. Res. **34**, 83 (2004)
18. J.A. Ascencio, P. Santiago, L. Rendon, U. Pal, Appl. Phys. A **78**, 5 (2004)
19. Hae Gwon Lee, Hee Chang Jeon, Tae Won Kang, Tae Whan Kim, Appl. Phys. Lett. **78**, 3319 (2001)
20. S.V. Zaitsev-Zotov, Yu A. Kumzerov, Yu A. Firsov, P. Monceau, J. Phys.: Condens. Matter **12**, L303 (2000)
21. S. Banerjee, A. Dan, D. Chakravorty, J. Mater. Sci. **37**, 4261 (2002)
22. K.A. Dick, K. Deppert, T. Martensson, B. Mandl, L. Samuelson, W. Seifert, Nano Lett. **5**, 761 (2005)
23. T. Bryllert, L.-E. Wernersson, L.E. Froerg, L. Samuelson, IEEE Electron Dev. Lett. **27**, 323 (2006)
24. E.I. Rashba, Sov. Phys. Solid State **2**, 1109 (1960)
25. Y.A. Bychkov, E.I. Rashba, JETP Lett. **39**, 78 (1984)
26. Y.A. Bychkov, E.I. Rashba, J. Phys. C **17**, 6039 (1984)
27. P. Pfeffer, W. Zawadzki, Phys. Rev. B **52**, 14332(R) (1995)
28. S. Datta, M. Das, Appl. Phys. Lett. **56**, 665 (1990)
29. S.D. Ganichev, V.V. Bel'kov, L.E. Golub, E.L. Ivchenko, Petra Schneider, S. Giglberger, J. Eroms, J. De Boeck, G. Borghs, W. Wegscheider, D. Weiss, W. Prettl, Phys. Rev. Lett. **92**, 256601 (2004)
30. V.A. Guzenko, J. Knobbe, H. Hardtdegen, Th. Schäpers, A. Bringer, Appl. Phys. Lett. **88**, 032102 (2006)
31. M. Governale, U. Zülicke, `arXiv:cond-mat/0407036` (2004)
32. E.A. de Andrada e Silva, G.C. La Rocca, Phys. Rev. B **67**, 165318 (2003)
33. W. Häusler, Phys. Rev. B **63**, 121310(R) (2001)
34. W. Häusler, Phys. Rev. B **70**, 115313 (2004)
35. Th. Schäpers, J. Knobbe, V.A. Guzenko, Phys. Rev. B **69**, 235323 (2004)
36. V. Gritsev, G. Japaridze, M. Pletyukhov, D. Baeriswyl, Phys. Rev. Lett. **94**, 137207 (2005)
37. M.G. Pala, M. Governale, U. Zülicke, G. Iannaccone, Phys. Rev. B **71**, 115306 (2005)
38. F. Mireles, G. Kirczenow, Phys. Rev. B **64**, 024426 (2001)
39. L.G. Wang, K. Chang, K.S. Chan, J. Appl. Phys. **99**, 043701 (2006)
40. X.F. Wang, Phys. Rev. B **69**, 035302 (2004)
41. Al.L. Efros, M. Rosen, Phys. Rev. B **58**, 7120 (1998)
42. X.W. Zhang, Y.H. Zhu, J.B. Xia, J. Phys.: Condens. Matter **18**, 4945 (2006)
43. J.M. Luttinger, Phys. Rev. **102**, 1030 (1956)
44. X.W. Zhang, J.B. Xia, Phys. Rev. B **72**, 075363 (2005)
45. Landolt-Börnstein, Group III, **17** a
46. X.W. Zhang, J.B. Xia, Phys. Rev. B **74**, 075304 (2006)